Int J Clin Exp Med 2017;10(9):13245-13253
www.ijcem.com /ISSN:1940-5901/IJCEM0049391

Original Article

Applied anatomy of maxillary sinus in cynomolgus monkeys: a CBCT study

Wangxi Wu[1*], Qi Zhang[1*], Xiao Hu[1*], Zhusu Chen[2], Lei Zhou[1]

Departments of [1]Implantology, [2]Endodontology, The Affiliated Stomatological Hospital of Southern Medical University, Guangdong Provincial Stomatological Hospital, Southern Medical University, Guangzhou 510280, P. R. China. [*]Equal contributors.

Received January 21, 2017; Accepted July 28, 2017; Epub September 15, 2017; Published September 30, 2017

Abstract: Objective: This study is to investigate possibility of usingcynomolgus monkeys as models to provide theoretical reference for maxillary sinus related scientific research of non-human primates. Methods: Cone bean CT (CBCT) scanning was performed in 20 sides of maxillary sinus from 10 cynomolgus monkeys. Measurements were conducted with the occlusal plane of bilateral maxillary first premolar to second molar as reference positions. The following distances were measured: from the corner of the anterior lower boundary in the lateral window of MSs to the anterior wall of the MS (d1); from the lower boundary to the maxillary sinus floor (d2); from the lower boundary to the top of alveolar ridge (d3); from the upper boundary to the top of alveolar ridge (d4); vertical window height (d5, d4-d3); anteroposterior window width (d6); the average thickness of the bone wall at anterior boundary (d7); the thickness of bone wall at 1/2 under the posterior boundary (d8); and the thickness of bone wall at the posterior upper corner of the window (d9). The mean value and standard deviation was then calculated. Results: No significant variations were found in the measured data of all individuals. And window position showed repeatability, suggesting a feasibility of the fenestration operation at the side wall of maxillary sinus. Conclusion: Cynomolgus monkey can be used for experimental model of lateral window approach.

Keywords: Cynomolgus monkey, maxillary sinus floor augmentation, lateral wall, applied an atomy, cone beam CT

Introduction

Primates, similar to human beings, are recently used as animal models in research. Previously, maxillary sinus floor augmentation (MSFA) was studied by using short-tailed macaques [1-4], however, the reported studies are limited in surgical methods and osteogenic efficiency, and did not mention detailed preoperative evaluation for the maxillary sinus (MS) of experimental animals or anatomic analysis. Therefore, these previous studies could not determine whether the surgery is different from clinical particularity.

Cynomolgus monkeys (CM), as common experimental animals in medicine, have a larger size and a skull size closer to human beings compared with short-tailed macaques, and are applied for various medical experiments [5, 6], especially for the experimental model of craniofacial surgery [7-9]. In a research using Cone bean CT (CBCT) to study Japanese macaques, scholars have demonstrated the differences in MS among distinct subtypes of local monkey species, however, no exploratory analysis of the anatomical structures of the lateral wall of maxillary sinus was performed [10]. Compared with other primates, CM has a potential to be an ideal animal model for MSFA due to their one litter per year, rapid reproduction, and abundant quantity of experimental animals. However, no relevant studies on the evaluation of MSFA via lateral wall in CM by using cone bean CT (CBCT) have been reported so far. Therefore, the present study aims to elaborate the anatomical structures of the maxillary sinus in CM by using CBCT scanning, and to explore the feasibility of CM as an animal model in MSFA via the lateral window approach.

Materials and methods

Experimental animals

A total of 10 male CMs (age range, 8-9 years; weight range, 7.3-9.3 kilograms) provided by

Guang Dong Blooming-Spring Biological Technology Development Co., Ltd in China, were enrolled in this study. The study received the approval from the Animal Experiment Ethics Committee of Southern Medical University and the Animal Experiment Ethics Committee of the Guangdong Laboratory Animals Monitoring Institute.

Animal anesthesia and posture preparation

Animal general anesthesia was performed with an intramuscular injection of 0.05 mg/kg atropine, 0.5 mg/kg xylazine, and 10 mg/kg ketamine till a completely inactive state. In the standing position, the body was fixed in the special examination chair by using cotton bandages, with the head forward and the mental region (namely the mandible) located in the examining table. The scanning detection was conducted by adjusting experimental animals to the occlusal plane of maxillary back teeth parallel to the ground and midline and interpupillary line located with examination equipment. After examinations, by an intramuscular injection of 1 mg/kg benzoxazole, the experimental animals gradually regained consciousness from eyes-open, the activity of the four limbs, to standing.

Design of MSFA via the lateral window approach

As for the design of the lateral window approach, briefly, the mesiodistal diameter of maxillary second molars was taken as the mesiodistal distance of the window, and the occlusal plane over the maxillary first premolar to the second molar was considered as reference plane. The lower boundary was the projection line at 1.5 mm above the molar root tip parallel to the reference plane and the upper boundary was the projection line at 1.5 mm below the infraorbital foramen parallel to the reference plane. The 1/2 segment under the posterior boundary was the projection line through the contact point on the distoproximal surface of the maxillary second molars and vertical to the reference plane, and the 1/2 segment above the posterior boundary presented a circular arc upwards and forwards to join with the upper boundary resulting from avoiding the zygomatic process.

The measurement of the distance for each animal was shown in **Figure 1** including the distance from the corner of the anterior lower boundary in the lateral window of maxillary sinus to the anterior wall of the MS (d1; a total of 2 data were measured at the left and the right side of MS respectively), the maximum distance from the lower boundary to the MS floor (d2; a total of 2 data were measured at the left and the right side of MS respectively), the distance from the lower boundary to the top of alveolar ridge (d3; a total of 4 data were measured at the left and the right mesiodistal maxillary second molars respectively), the distance from the upper boundary to the top of alveolar ridge (d4; a total of 2 data were measured at the left and the right side of MS respectively), vertical window height (d5, d4-d3), anteroposterior window width (d6; the distance between the contact points on the mesiodistal surface of the maxillary second molars; a total of 2 data were measured at the left and the right side respectively), the average thickness of the bone wall at anterior boundary (d7; the thickness of the bone wall from two end points of the anterior boundary to the midpoint of the anterior boundary was measured; a total of 6 data were measured at the left and the right sides respectively), the thickness of bone wall at 1/2 under the posterior boundary (d8; the thickness of the bone wall from the lower end point of the posterior boundary to the midpoint of the posterior boundary was measured; a total of 4 data were measured at the left and the right sides respectively), and the thickness of bone wall at the posterior upper corner of the window (d9; the thickness of the bone wall at the front of the zygomatic arch of the upper boundary was measured; a total of 2 data were measured at the left and the right side respectively).

CBCT images

The examination was performed using cone beam computed tomography (NewTomVGi, Italy), Images of the maxillary sinus and surrounding structures were acquired from each sample. The tomography specification applied was as follows: tube potential (kV) 110, tube current (mA) 3, high-resolution images cylindrical areas 15×12 cm^2, reconstruction time(s) <30, Voxel size (mm) 0.150, Exposure time(s) 1.8. Image analysis was performed on the NNT Viewer version 5.5 (Installation package 5.5.0 NewTom Cone Bean 3D Imaging) software, and on a multiplanar reconstruction window in

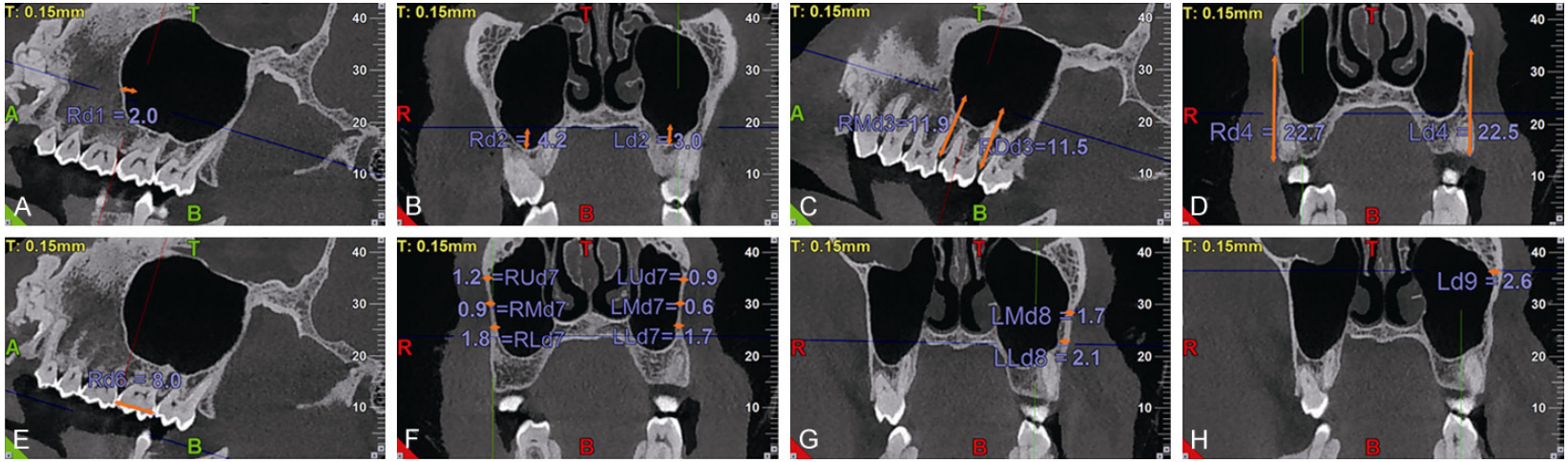

Figure 1. The measurement CBCT data of maxillary sinus in cynomolgus monkey. (A) from the corner of the anterior lower boundary in the lateral window of MSs to the anterior wall of the MS (d1); from the lower boundary to the maxillary sinus floor (d2); from the lower boundary to the top of alveolar ridge (d3); from the upper boundary to the top of alveolar ridge (d4); vertical window height (d5, d4-d3); anteroposterior window width (d6); the average thickness of the bone wall at anterior boundary (d7); the thickness of bone wall at 1/2 under the posterior boundary (d8); and the thickness of bone wall at the posterior upper corner of the window (d9).

Table 1. Measurements data of maxillary sinus in cynomolgus monkey*

d1	d2	d3	d4	d5	d6	d7	d8	d9
2.5±1.0	3.1±1.1	11.5±1.5	21.5±1.3	10.0±2.3	8.2±0.4	1.9±0.9	3.6±1.4	3.1±1.4

*The distance (mm), mean ± SD.

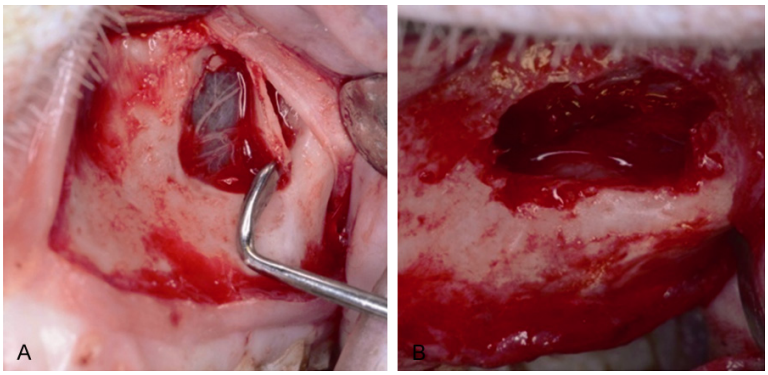

Figure 2. Maxillary sinus surgery. A. After the bone window was opened, the thin mucosa displayed and showed high tension; B. After complete mucosal elevation, the maxillary sinus floor plate was exposed and mucosa tension decreased.

which the axial, coronal, and sagittal planes could be visualized in 0.15 mm intervals.

Statistical analysis

All data were entered into a database system and evaluated using SPSS version 17.0 (SPSS Inc., Chicago, IL, USA). All data in this study were presented as mean ± SD. Sample data were analyzed anonymously. Each case was assigned a resistration number before evaluation to allow for explicit and anonymous attribution of the necessary information. Intra-examiner agreement was determined by comparing two repeated measurements of 2 randomly selected cross-sectional images. The data analysis was performed with descriptive statistics.

Results

CBCT analyzation and measurement of maxillary sinus

In order to measure the values of animals' maxillary sinus related to anatomy, CBCT was performed. Among the 20 sides of maxillary sinus of 10 animals, d1 ranged from 1.1 to 4.6 mm (**Figure 1A**), d2 was 1.0 to 4.7 mm (**Figure 1B**), with the mean value of 2.5±1.0 mm and 3.1±1.1 mm (**Table 1**) respectively, indicating that the anterior and lower boundaries could be well separated. The length of d3 was between 8.2 and 14.5 mm (**Figure 1C**), d4 was from 19 to 23.3 mm (**Figure 1D**), and d5=d4-d3 ranged from 6.55 to 13.3 mm, with the mean of 10.0±2.3 mm (**Table 1**), demonstrating that the vertical height of the window could support the convenience subsequent operation. The mean of the window anterior-posterior width defined as d6 was 8.2±0.4 mm (**Table 1**), with the range of 7.7 to 9.2 mm, resulting in the standard deviation of 0.4 mm. The collected d6 data were of the most constant in all of data groups, which also supported the convenience subsequent operation. The thicknesses of the lower 1/2 and upper points of posterior boundary were 3.6±1.4 mm and 3.1±1.4 mm (**Table 1**) respectively, and compared with the thickness of anterior boundary (1.9±0.9 mm) (**Table 1**), the posterior boundary was thicker, however, it still could be dealt with uneventfully. Together, the measured data of CBCT indicated that the window place we designed was relatively repeatable.

Maxillary sinus membrane

All of the sections in 20 cavities could not catch the sinus membrane in CBCT. This was due to the film-like membrane tightly attached on bone walls, additionally, the minimal voxel size of the device was 0.15 mm and the thickness of membrane might be less than the min-size. To further investigate the situation of maxillary sinus membrane, applied anatomy of cranial bone was performed. Once exposed, direct-viewing showed that the maxillary sinus membrane was as thin as dragonfly wings samples, with small amount of bundle connective tissue and blood capillary, presenting a tight tension (**Figure 2A**). The sinus membrane thickened with tension decrease by separating from bone wall and lifting toward cavity (**Figure 2B**). To

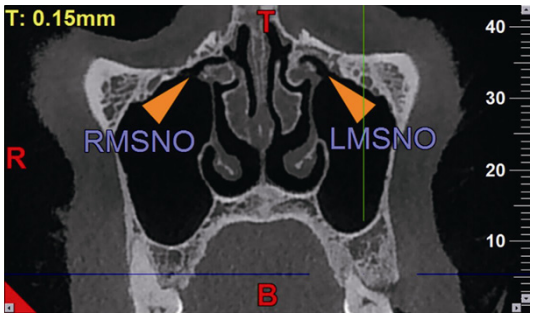

Figure 3. Bilateral maxillary sinus cleft was made from the posterior wall of the medial wall of the maxillary sinus through the lateral nasal wall drainage to the nasal meatus.

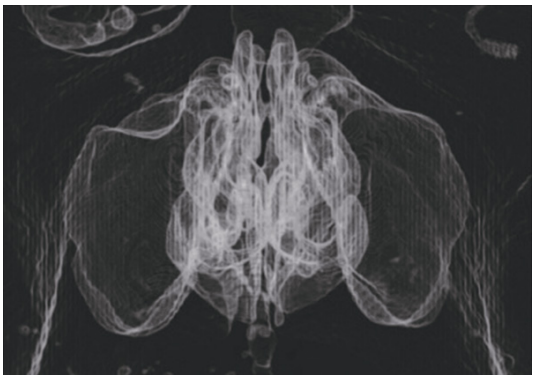

Figure 4. Three-dimensional image reconstruction showed that maxillary sinus of cynomolgus monkey was inverted cone.

sum up, the results argued that animal sinus membrane cannot be detected by CBCT and it lines on sinus cavity bone surface smoothly.

The relationship between maxillary sinus and adjacent anatomy structures

In order to avoid the complications as result of injuring the adjacent anatomy structures or teeth, relationship between maxillary sinus and adjacent anatomy structures was investigated. As illustrated in **Figure 3**, the sinus natural ostium almost locates on the top of inside wall of sinus to the outside wall of nasal cavity between distal part of the first molar and mesial part of the second molar drainage to middle nasal meatus in coronary section. Almost all tips of molar root protruded forward to sinus floor except 2 sides sinus in an animal, confirmed the anterior-posterior range of the maxillary sinus floor extending from the first to third molar (**Figure 1C**). In line with this, the designed window place is safe enough to avoid the complications after surgery.

Three dimensional imaging of maxillary sinus

To further afford more information of practicability of cynomolgus monkeys, the anatomical data was compared with that of human beings. Three dimensional images of cynomolgus monkey maxillary sinus cavity displayed as vertebral shaped hole cavity (**Figure 4**). **Figure 5** showed local reconstruction images of sinus cavity viewed from different angles. Briefly, the appearance of maxillary sinus in cynomolgus monkeys showed square circular. Measured imaging data of cynomolgus monkey and human maxillary sinus cavity diameter were 23.3 mm and 28.7 mm (as shown in **Table 2**), and the anteroposterior diameter of cynomolgus monkey maxillary sinus was about 4/5 to that of human beings. In addition, the widths between buccal wall and nasal wall of maxillary sinus of the two species were 12.5 mm and 16.2 mm, with the ratio close to 0.8. The height between the top wall and sinus floor of maxillary sinus in cynomolgus monkeys and humans were 17.8 mm and 29 mm, with a ratio close to 0.6, which was consistent with the body shape of the two species. Compared with the human beings, the ratio of longitudinal figure to transverse shape in cynomolgus monkeys was obviously reduced, therefore, its maxillary sinus shape is seen as an overall reduction of the human maxillary sinus. From the angle standpoint, the cleft of the maxillary sinus, located in the nasal side wall, is closer to the bottom of the maxillary sinus in cynomolgus monkeys, which, is more conducive to sinus drainage. As a result, it has much healthy maxillary sinus mucosa, and hence, no inflammatory thickening of the mucosa is seen by the 0.15 mm thickness CBCT image. Collectively, the physiological and anatomical characteristics of cynomolgus monkeys are close to that of humans.

Discussion

MSFA via the lateral window approach can achieve an effective bone augmentation, which facilitates the clinical extensive development of implant treatment for bone defects in the maxillary posterior region [11-14], however, the exact osteogenesis mechanism within the lifting space still needs further exploration [13-15], especially the osteogenic capacity of the sinus membrane (SM) of raises different viewpoints. In the study of short-tailed macaques [1], it has been observed that MSFA using the lateral approach combined with homochronous

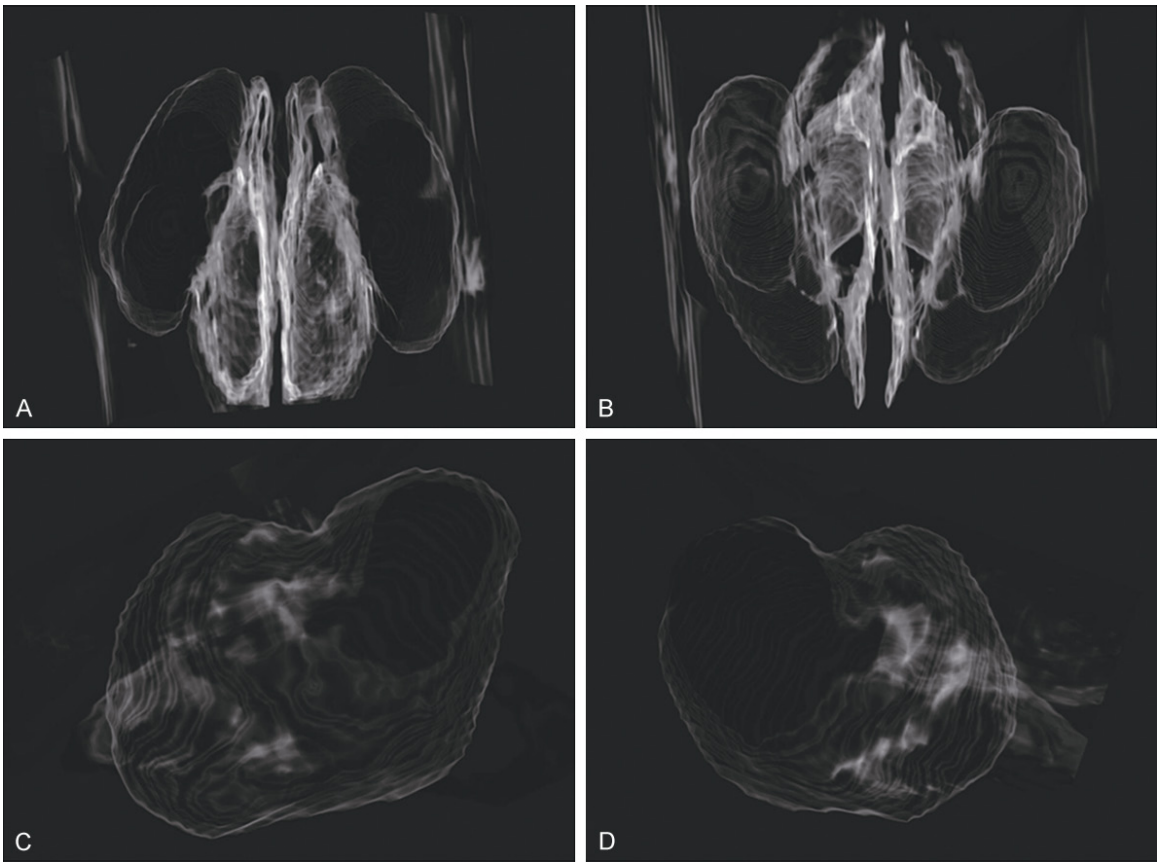

Figure 5. The highlightingmaxillary sinus three dimensional imagesof cynomolgus monkey from different views. Anterior (A), top (B), left (C) and right (D) views.

Table 2. The maxillary sinus dimension comparision between CM and Human (n=10)

$d_{A-P}d_{T-B}$	d_{B-N}	V		
Cynomolgus	23.3±1.1	17.8±1.8	12.5±1.6	4.1±0.90
Human	28.7±1.6	29.0±1.9	16.2±1.0	12.6±1.2

Note: d= $\bar{x}$ ±sd (mm) V= $\bar{x}$ ±sd (L); d_{A-P}: the distance between anterior to posterior wall in maxillary sinus; d_{T-B}: the distance between top to bottom in maxillary sinus; d_{B-N}: the distance between buccal to nasal wall in maxillary sinus; V: volumn of maxillary sinus.

implant placement leads to the presence of osteogenic properties in SM. In addition, a study on newly similar animals proposed that MSFA from lateral wall combined with homochromous implant placement resulted in no new bone formation between SM and implants, which denied the osteogenic properties of SM [3]. However, it has been shown clinically that lateral wall MSFA combined with blood filling instead of grafting could obtain significant bone augmentation in the space maintained by blood filling, supporting the osteogenic potential of SM [14]. Moreover, some scholars isolated stromal stem cells from SM with the ability to form bone-like tissue [15], and conducted a homochronous in vivo experiment on dogs revealing a weak osteogenic ability in SM as compared with the bone wall [16]. Obviously, there are still controversies on the osteogenic ability of SM after sinus lifting.

MSFA by lateral wall is a standard experimental method for SM, and setting effective anatomical markers as reference as well as designing accurate window location and size are prerequisites for successful open of the lateral bone window of the MS and separation and lifting of the SM. The anatomic structure and physiological functions of primates are almost in line with human beings, and is the optimal experimental model for the study of SM. However, the body shape and anatomical-morphology characteristics of primates with different subtypes present many similarities and dif-

ferences; thus imaging assessment is necessary before model construction. In the present study, through CBCT scanning, MS showed a vertebral body cavity in three-dimension (**Figure 4**), and sinus floor, extended from the lateral nasal wall towards the alveolar process, was a buccal thin bone plate covering the root surface and adjacent to maxillary molar root tip. These characteristics were similar to human beings and therefore the results of the animal model will be more close to those in clinic. Additionally, maxillary second molars were taken as reference position and the occlusal plane from premolars to molars as reference plane, a lateral window approach above the molar root tip, below the infraorbital foramen, posterior to the front wall of maxillary sinus, and anterior lower to the zygomatic arch was obtained. This ensured the possibility for further exploring the potential mechanisms of later osteogenesis in sinus.

In the past, some scholars performed a maxillary sinus augmentation via the lateral window approach in rhesus monkeys [17], from a window with a small area gradually enlarging to a rectangular window with a width of 10 mm and a length of 5 mm. The same as rhesus monkeys, CMs applied in this study are belonging to primates, however, CMs had a smaller body shape and slightly different window from CBCT data compared with that of rhesus monkeys. The anterior boundary was 2.5±1.0 mm from the front wall of sinus, the lower boundary above root tip was about 1.5 mm and 3.1±1.1 mm from the sinus floor at most, the upper boundary adjacent to the infraorbital foramen was about 1.5 mm, and the posterior boundary was adjacent to the zygomatic process, therefore, further range enlargement was relatively limited. Moreover, the detection values were maximum boundaries within the operable range and if there were experimental devices to be placed into the sinus cavity during surgery, the operation should be performed within this measuring range. This would ensure successful and complete SM lifting with windowing, and favor the observation of experimental results.

Previously, a team reported a study on capuchin monkeys with a window width of 10 mm and a height of 6 mm [1]. Homochronous placement of implant during augmentation by lateral window and presurgerical evaluation of window design using CBCT were performed. This demonstrated the necessity of three-dimensional imaging examination before this kind of experiments, however, there was no further description of imaging data in this study. Subsequently, this team reported a window area (width, 8 mm; height, 6 mm), which is similar to their previously described study, and no presurgerical imaging examination was performed [2, 18]. During the same period, other research group[4] also reported a window design with same area. The window values in the MSFA through the lateral window access of the above primates are similar; in our present study, definition was conducted only in reference anatomic landmarks but not in values for window design. Our measuring results of 10×8.2 mm support previous experiments, and meanwhile significantly enhance the prejudgment of operative procedure for experimenters. The imaging data of d1=2.5±1.0 mm and d2=3.1±1.1 mm in this study demonstrated the feasibility of window design. The osteogenesis of SM can also be observed from 4 surfaces: the mesial, distal, inner, and the top for comparisons. The measuring data of the bone wall thickness of the anterior boundary was 1.9±0.9 mm, the 1/2 segment under the posterior boundary was 3.6±1.4 mm, and the posterior upper corner of the window was 3.1±1.4 mm, suggesting that the thickness of the bone wall of the maxillary sinus was moderate and was suitable for successful windowing operation. In addition, imaging examination revealed that the bone wall of the window tend to be thinner towards the center, therefore reduced window area was more helpful to windowing operative procedure. It is recommended that the windowing procedure can be performed from a small window in the center and gradually enlarge outwards. In addition, a complete windowing with a direct determination of eventual boundaries of the window is also suggested.

The distance from the lower boundary to the top of alveolar ridge and the distance from the upper boundary to the top of alveolar ridge in this study suggested an effectiveness of the selection of anatomic reference structure. The data of vertical window height and anteroposterior window width implicated a good repeatability of window design. A high repeatability was found in experimental operation according to this method of window design. Moreover, after opening the square-round-shaped bone window, the tight SM was exposed and separated

along the maxillary sinus floor and the anterior wall. And thereby osteogenic space was obtained with complete lifting, revealing the lifted SM inner side within the window and the smooth bone surface of maxillary sinus floor.

Conclusion

In summary, setting maxillary second molars of CMs and the occlusal plane of maxillary premolars and molars as references facilitated the assessment of the anatomical structures of the maxillary sinus. Determining lateral window approach of the maxillary sinus with molar root tip, infraorbital foramen, and zygomatic arch contributed to operability and repeatability in maxillary sinus floor augmentation. All designs were confirmed by CBCT analyzation and measurement. Therefore, CMs can be used to construct an ideal experimental model for maxillary sinus floor augmentation via the lateral window approach.

Acknowledgements

This work is supported by grants from National Natural Science Foundation of China (No. 81170998) and Medical Science Research Foundation of Guangdong Province (C2012034). We gratefully acknowledge the help of all the colleagues of Radiology Department of Guangdong Provincial Stomatological Hospital for providing CBCT scanning. Additionally, we appreciate the help of the experimental animal groups of the Guangdong Institute of Animal Experiments for technical support.

Disclosure of conflict of interest

None.

Address correspondence to: Lei Zhou, Department of Implantology, The Affiliated Stomatological Hospital of Southern Medical University, Guangdong Provincial Stomatological Hospital, Southern Medical University, 366 S, Jiangnan Boulevard, Guangzhou 510280, P. R. China. Tel: +86-20-84233801; Fax: +86-20-84233801; E-mail: zho668@263.net

References

[1] Palma VC, Magro-Filho O, de Oliveria JA, Lundgren S, Salata LA, Sennerby L. Bone reformation and implant integration following maxillary sinus membrane elevation: an experimental study in primates. Clin Implant Dent Relat Res 2006; 8: 11-24.

[2] Cricchio G, Palma VC, Faria PE, de Olivera JA, Lundgren S, Sennerby L, Salata LA. Histological outcomes on the development of new space-making devices for maxillary sinus floor augmentation. Clin Implant Dent Relat Res 2011; 13: 224-30.

[3] Scala A, Botticelli D, Faeda RS, Garcia RI, Americo DO, Lang NP. Lack of influence of the Schneiderian membrane in forming new bone apical to implants simultaneously installed with sinus floor elevation: an experimental study in monkeys. Clin Oral Implants Res 2012; 23: 175-81.

[4] Schweikert M, Botticelli D, de Oliveira JA, Scala A, Salata LA, Lang NP. Use of a titanium device in lateral sinus floor elevation: an experimental study in monkeys. Clin Oral Implants Res 2012; 23: 100-5.

[5] Liedigk R, Kolleck J, Böker KO, Meijaard E, Md-Zain BM, Abdul-Latiff MA, Ampeng A, Lakim M, Abdul-Patah P, Tosi AJ, Brameier M, Zinner D, Roos C. Mitogenomic phylogeny of the common long-tailed macaque (Macaca fascicularis fascicularis). BMC Genomics 2015; 16: 222.

[6] Lu W, Hu H, Sevigny J, Gabelt BT, Kaufman PL, Johnson EC, Morrison JC, Zode GS, Sheffield VC, Zhang X, Laties AM, Mitchell CH. Rat, mouse, and primate models of chronic glaucoma show sustained elevation of extracellular ATP and altered purinergic signaling in the posterior eye. Invest Ophthalmol Vis Sci 2015; 56: 3075-83.

[7] Hanisch O, Tatakis DN, Rohrer MD, Wohrle PS, Wozney JM, Wikesjo UM. Bone formation and osseointegration stimulated by rhBMP-2 following subantralaug mentation procedures in nonhuman primates. Int J Oral Maxillofac Implants 1997; 12: 785-92.

[8] Omran M, Min S, Abdelhamid A, Liu Y, Zadeh HH. Alveolar ridge dimensional changes following ridge preservation procedure: part-2 - CBCT 3D analysis in non-human primate model. Clin Oral Implants Res 2016; 27: 859-66.

[9] Piccinini M, Rebaudi A, Sglavo VM, Bucciotti F, Pierfrancesco R. A new HA/TTCP material for bone augmentation: an in vivo histological pilot study in primates sinus grafting. Implant Dent 2013; 22: 83-90.

[10] Zaizen T, Sato I, Miwa Y, Sunohara M, Yosue T, Mine K, Koseki H, Shimada K. Differences in the morphology of the maxillary sinus and roots of teeth between Macacafuscata and Macacafuscatayakui determined using cone beam computed tomography. Okajimas Folia Anat Jpn 2013; 89: 125-30.

[11] Riben C, Thor A. Follow-Up of the sinus membrane elevation technique for maxillary sinus implants without the use of graft material. Clin Implant Dent Relat Res 2016; 18: 895-905.

[12] Bensaha T, El MH. Evaluation of new bone formation after sinus augmentation with two different methods. Int J Oral Maxillofac Surg 2016; 45: 93-8.
[13] Markovic A, Misic T, Calvo-Guirado JL, Delgado-Ruiz RA, Janjic B, Abboud M. Two-center prospective, randomized, clinical, and radiographic study comparing osteotome sinus floor elevation with or without bone graft and simultaneous implant placement. Clin Implant Dent Relat Res 2016; 18: 873-82.
[14] De Oliveira GR, Olate S, Cavalieri-Pereira L, Pozzer L, Asprino L, de Moraes M, de Albergaría-Barbosa JR. Maxillary sinus floor augmentation using blood without graft material. Preliminary results in 10 patients. J Oral Maxillofac Surg 2013; 71: 1670-5.
[15] Pasquali PJ, Teixeira ML, de Oliveira TA, de Macedo LG, Aloise AC, Pelegrine AA. Maxillary sinus augmentation combining bio-oss with the bone marrow aspirate concentrate: a histomorphometric study in humans. Int J Biomater 2015; 2015: 121286.
[16] Rong Q, Li X, Chen SL, Zhu SX, Huang DY. Effect of the schneiderian membrane on the formation of bone after lifting the floor of the maxillary sinus: an experimental study in dogs. Br J Oral Maxillofac Surg 2015; 53: 607-12.
[17] El-Madany I, Emam H, Sharawy M. Comparison of cellular response to anorganic bone matrix/cell binding peptide and allogenic cranial bone after sinus augmentation in rhesus monkeys. J Oral Implantol 2011; 37: 233-45.
[18] Cricchio G, Palma VC, Faria PE, de Oliveira JA, Lundgren S, Sennerby L, Salata LA. Histological findings following the use of a space-making device for bone reformation and implant integration in the maxillary sinus of primates. Clin Implant Dent Relat Res 2009; 11 Suppl 1: e14-22.